Journal of Magnetic Resonance **137,** 100–107 (1999)
Article ID jmre.1998.1633, available online at http://www.idealibrary.com on IDEAL®

PRAWN: Mixing Sequences for Selective Heteronuclear *J* Cross Polarization

N. Chandrakumar[1] and R. Kimmich

Sektion Kernresonanzspektroskopie, Universität Ulm, D-89069 Ulm, Germany

Received February 19, 1998; revised August 31, 1998

In this work, we present a family of pulse sequences for selective heteronuclear *J* cross-polarization (*J*CP), which we have developed especially for indirect ^{13}C imaging using *J*CP, for example in the CYCLCROP environment. The sequences are straightforward to implement and operate reliably. Results of an average Hamiltonian analysis are given for the basic sequence, which we term PRAWN (pulsed rotating frame transfer sequence with windows). It is shown experimentally that the pulse sequence, which operates efficiently with low RF duty cycles down to a few percent, has a useful tolerance range to absolute Hartmann–Hahn mismatch and generates coherence transfer spectra in close correspondence with the *J*CP average Hamiltonian. Computer simulation of the performance of the basic sequence on a heteronuclear spin-$\frac{1}{2}$ AX system is also presented. The mismatch compensation of PRAWN may be markedly enhanced further by issuing a π pulse to each spin halfway through the basic PRAWN train and in phase quadrature to it. A simple analysis of this modified sequence, PRAWN-π, is given under conditions of mismatch and off-resonance irradiation.

Key Words: **indirect ^{13}C imaging using CYCLCROP; selective heteronuclear *J* cross-polarization; Hartmann–Hahn mismatch; pulsed rotating frame transfer sequences with windows; density matrix theory of mismatch compensation and off-resonance effects.**

INTRODUCTION

We have been interested in the proton detected indirect imaging of ^{13}C in elastomers and in plants *in vivo*, employing the cyclic cross-polarization scheme, CYCLCROP (*1*). Our approach relies on introducing a ^{13}C-enriched species as tracer for the application in view (*2, 3*). In this context, we have developed a family of simple mixing sequences to effect the desired selective *J* cross-polarization for such applications. Our pulse sequence family, which we term pulsed rotating frame transfer sequences with windows (PRAWN), may be used with both single-coil and two-coil probeheads, permits operation with very low average RF field amplitudes of the order of the coupling in question, *J*, and is robust in operation, besides being tolerant to Hartmann–Hahn mismatch (*4–10*). In this report, we present the basic characteristics of PRAWN, including a simple variant, PRAWN-π.

[1] On leave from: Laboratory of Chemical Physics, Central Leather Research Institute, CSIR, Adayaru, Chennai–600 020, Tamil Nadu, India.

BASIC SEQUENCE

The basic PRAWN sequence consists simply of a series of RF pulses with constant pulse duration (τ_w), flip angle (θ), and phase (say x), as well as constant pulse interval (τ_s), issued on both spins simultaneously. The sequence is depicted in Fig. 1.

The operation of the sequence may be readily understood on the basis of an average Hamiltonian analysis of a cycle of n pulses of the sequence satisfying the condition

$$n\theta = 2\pi. \qquad [1]$$

We find on applying the standard treatment following Ellett and Waugh (*11*) that the zeroth-order average offset Hamiltonian vanishes:

$$n(\tau_s + \tau_w)(I_z)_{av} = 0. \qquad [2]$$

This result is independent of the sequence parameters, except for the case $\theta = 2\pi$, for which we find:

$$(\tau_s + \tau_w)(I_z)_{av} = \tau_s I_z. \qquad [3]$$

Clearly, Eq. [3] takes the same form as Eq. [2] for the case $\tau_s = 0$, which is equivalent to cw irradiation.

For the zeroth-order average coupling Hamiltonian, we find, for $I = \frac{1}{2} = S$:

$$\bar{H} = \pi J(I_z S_z + I_y S_y). \qquad [4]$$

This form is once again independent of the sequence parameters, except for the two cases $\theta = \pi$ and $\theta = 2\pi$, for which we find

$$n(\tau_s + \tau_w)(I_z S_z)_{av} = n\,\frac{\tau_w}{2}\,(I_z S_z + I_y S_y) + n\tau_s I_z S_z. \qquad [5]$$

1090-7807/99 $30.00

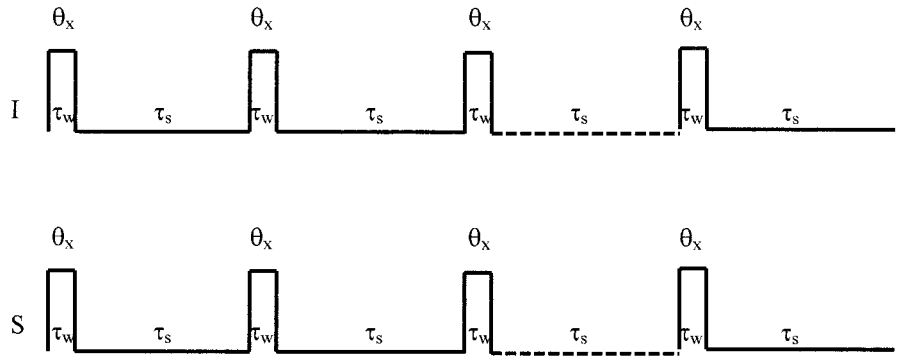

FIG. 1. Schematic of the pulsed rotating frame transfer sequence with windows (PRAWN).

Once again, Eq. [5] takes the same form as Eq. [4] for the case $\tau_s = 0$, which is equivalent to cw irradiation.

EXPERIMENTAL TESTS AND COMPUTER SIMULATIONS

In its basic version, we normally employ PRAWN with an RF amplitude of ~500 Hz to 1 kHz and a duty cycle ($\tau_w/(\tau_w + \tau_s)$) of about 20% (corresponding to an average RF amplitude of 100–200 Hz), typically covering the mixing period with one cycle of the sequence for transfer mediated by a $^1J_{C\text{-}H}$ coupling. The experimental coherence transfer spectrum of Fig. 2 clearly demonstrates the expected behavior.

At this level, PRAWN exhibits a useful tolerance range to *absolute* Hartmann–Hahn mismatch, since there are infinitely many solutions for θ satisfying cyclicity, and in particular the low flip angle solutions cluster closely together. Equivalently, one may view the absolute mismatch tolerance range of the basic version of PRAWN as related to that of cw *J*CP scaled up by the inverse of the duty cycle factor of the sequence, $((\tau_w + \tau_s)/\tau_w)$. This can be handy in terms of convenience for setup, although the *relative* mismatch tolerance ($\omega_{1I} - \omega_{1S}/\omega_1$) is identical to that for the cw case at the same *average* RF field amplitude. Experimental demonstration of the mismatch behavior is shown in Fig. 3. It may be noted further that unlike cw irradiation, and typically for a periodic pulse sequence, PRAWN exhibits sideband responses, which may be put to use.

To characterize further the behavior of PRAWN in comparison to cw *J*CP, we present in Fig. 4a the Antiope (*12*) simulation of the operation of the sequence applied on resonance with a 20% RF duty cycle to a heteronuclear spin-$\frac{1}{2}$ AX system ($J = 200$ Hz). The parameters we employed for the simulation closely relate to the typical experimental situation and are listed in the figure caption. The ^{1}H RF amplitude of the mixing pulses was incremented in 41 steps from 0.2 to 1.8 kHz to generate the simulation stack plot, the ^{13}C RF amplitude of the mixing pulses being held constant at 1 kHz. Figure 4b displays the performance

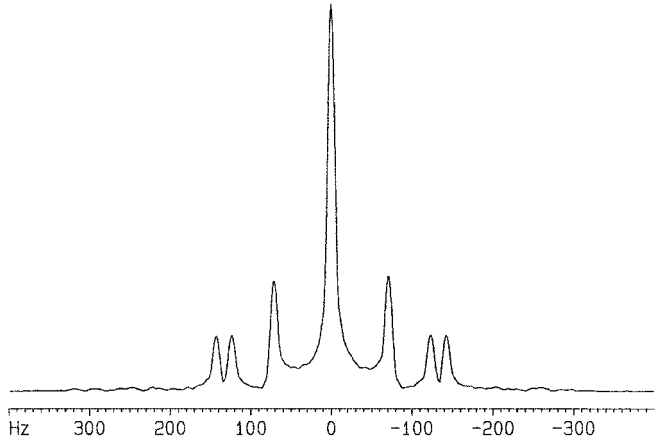

FIG. 2. Coherence transfer (CT) spectrum (F_1 projection) of the PRAWN sequence in forward mode ($X_3 \rightarrow A$, $^1H \rightarrow {}^{13}C$) obtained on the AX_3 methyl group of a sample of ^{13}C-enriched methanol ($J = 140$ Hz) by systematic incrementation of the total mixing time, i.e., the duration for which PRAWN cycles are issued. Peak RF field amplitude corresponded nominally to ~1 kHz (^{13}C RF attenuation corresponded to 6.8 dB and ^{1}H RF attenuation corresponded to 15.8 dB), while pulse widths τ_w were 50 μs and pulse intervals τ_s were 200 μs. The coherence transfer spectra in forward and reverse mode ($A \rightarrow X_3$, $^{13}C \rightarrow {}^1H$) correspond to the theoretical coherence transfer function for the AX_3 system:

$$\tfrac{5}{8} - \tfrac{1}{4}\cos(\pi Jt) - \tfrac{1}{4}\cos(\sqrt{3}\pi Jt) - \tfrac{1}{8}\cos(2\pi Jt).$$

Note that the CT spectrum in cyclic mode ($X_3 \rightarrow A$, saturate X_3, $A \rightarrow X_3$) corresponds to the square of this function. CT spectral amplitudes—and frequencies—are modified by Hartmann–Hahn mismatch. It may be noted that in addition to providing complete information concerning the amplitudes, phases, and frequencies of coherence transfer, linewidths of signals in the coherence transfer spectrum give an accurate measure of the relevant relaxation rates in the rotating frame. Should the details of CT for the individual multiplet components not be of interest, one could in principle conveniently acquire the CT spectrum in 1D mode by sampling during the windows of the PRAWN cycle. The experiments were run on a Bruker DSX 400 system, employing a homebuilt single-coil insert (doubly tuned to ^{13}C and ^{1}H) plugged into the standard microimaging probehead. Spectrum is displayed in magnitude mode; 128 t_1 increments, zero-filled to 512 points; F_1 spectral width 800 Hz. Both spins were irradiated on resonance. Note the three coherence transfer frequencies, as predicted for an AX_3 system.

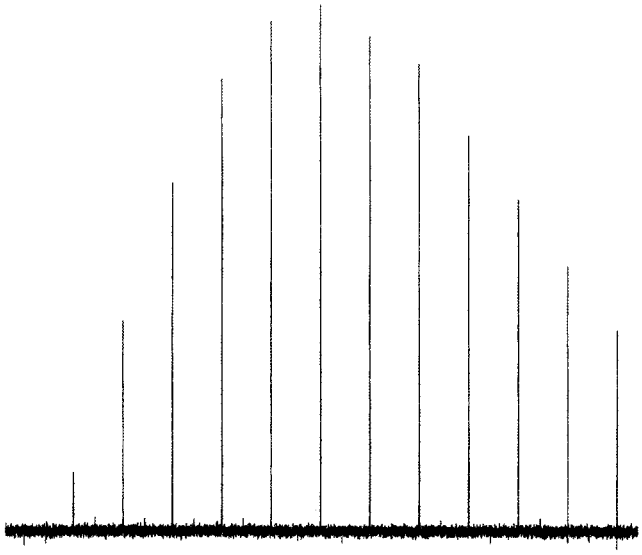

FIG. 3. Signal amplitude obtained with PRAWN in forward mode on sodium [2-^{13}C]acetate (J = 128 Hz), as a function of proton attenuator setting, varied from 13.0 to 25.0 dB (~1678 to 421 Hz peak RF amplitude), in 1.0-dB steps. Carbon attenuator was set to 10.0 dB, corresponding nominally to 1 kHz peak RF amplitude (note that the homebuilt probehead insert used for this and subsequent figures is different from the one used for Fig. 2). Both spins were irradiated on resonance with an 18-segment PRAWN pulse train whose pulse widths were 50 μs and pulse intervals 200 μs, constituting a total mixing period of 4.5 ms.

of cw *J*CP under related conditions, using a ^{13}C mixing RF amplitude of 200 Hz; the ^{1}H mixing RF amplitude was incremented in 41 steps from 0.04 kHz to 0.36 kHz in this case. These values are equivalent to the average RF amplitudes employed in the PRAWN simulation of Fig. 4a. The simulations establish the close correspondence on resonance, predicted on the basis of the average Hamiltonian analysis; further, the predicted amplification of the *absolute* cw mismatch tolerance range by the inverse of the duty cycle factor is verified for the basic PRAWN sequence, the *relative* mismatch tolerance range with respect to the average RF field amplitude being identical for the two cases as expected.

We point out that the operation of a simple train of identical pulses in effecting heteronuclear *J*CP was noticed earlier (*13*) but not explored further systematically. In the limit of small flip angles, the basic PRAWN sequence may be viewed as the heteronuclear analog of the DANTE sequence, which has been employed by Kupče and Freeman (*14*) for selective homonuclear Hartmann–Hahn transfer. Double selective homonuclear Hartmann–Hahn transfer employing amplitude modulation has also been reported by Bodenhausen *et al.* (*15*), while the relation of a pulse train to cw irradiation has been discussed by Kessler *et al.* (*16*) in the context of separating TOCSY from ROESY effects in homonuclear spin systems.

THE HARTMANN–HAHN MISMATCH COMPENSATED VERSION

The basic PRAWN sequence permits tuning of its behavior by simple means, including the insertion of π pulses at strategic locations. Consider, for instance, the situation resulting from the application of a simultaneous pair of π pulses in phase quadrature to the basic PRAWN pulse train, midway through the mixing period covered by two cycles of the sequence. This version of PRAWN, which we term PRAWN-π, exhibits a pronounced tolerance to Hartmann–Hahn mismatch, as demonstrated by the experimental spectra of Fig. 5.

To model the effect of mismatch, we first treat the on-resonance cw case, but include a Hartmann–Hahn mismatch contribution Δ to the Hamiltonian in the synchronized doubly rotating frame (SDRF), mismatch being related to the difference of RF field amplitudes ω_{1I} and ω_{1S}

$$\bar{H} = \pi J((I_y S_y + I_z S_z) + k(I_x - S_x)) \qquad [6]$$

$$k = \frac{\Delta}{2\pi J}; \quad \Delta = \omega_{1I} - \omega_{1S}. \qquad [7]$$

For purposes of later comparison, we recall that the relevant symmetric component of the density operator is conserved under this Hamiltonian, while the corresponding antisymmetric component evolves in time:

$$(I_x + S_x) \xrightarrow{\bar{H}t} (I_x + S_x)$$

$$(I_x - S_x) \xrightarrow{\bar{H}t} \frac{(4k^2 + c)}{(4k^2 + 1)} (I_x - S_x)$$

FIG. 4. (a) Antiope simulation of a CH system (on resonance, J = 200 Hz) subjected to the PRAWN sequence. A proton 90° $-x$ pulse of amplitude 10 kHz and duration 25 μs was followed by a PRAWN train on both spins, the train consisting of 20 repetitions of an 18° y pulse of RF amplitude 1 kHz and duration 50 μs, followed by an interval of 200 μs on the ^{13}C channel; on the ^{1}H channel, the same parameters were employed, except that the RF amplitude (and therefore the flip angle) was varied on successive runs, in 41 equally spaced steps from 200 to 1800 Hz. The simulations were performed on a Pentium 166 MMX PC with Version 1.44 of the software. The stack plot displays the amplitude of the carbon y magnetization. (b) Antiope simulation of the CH system of (a), irradiated cw. All sequence parameters were the same as for (a), except that the cw irradiation, of duration 5 ms, had a fixed amplitude of 200 Hz on the ^{13}C channel, while the ^{1}H channel amplitude was varied on successive runs, in 41 equally spaced steps from 40 to 360 Hz.

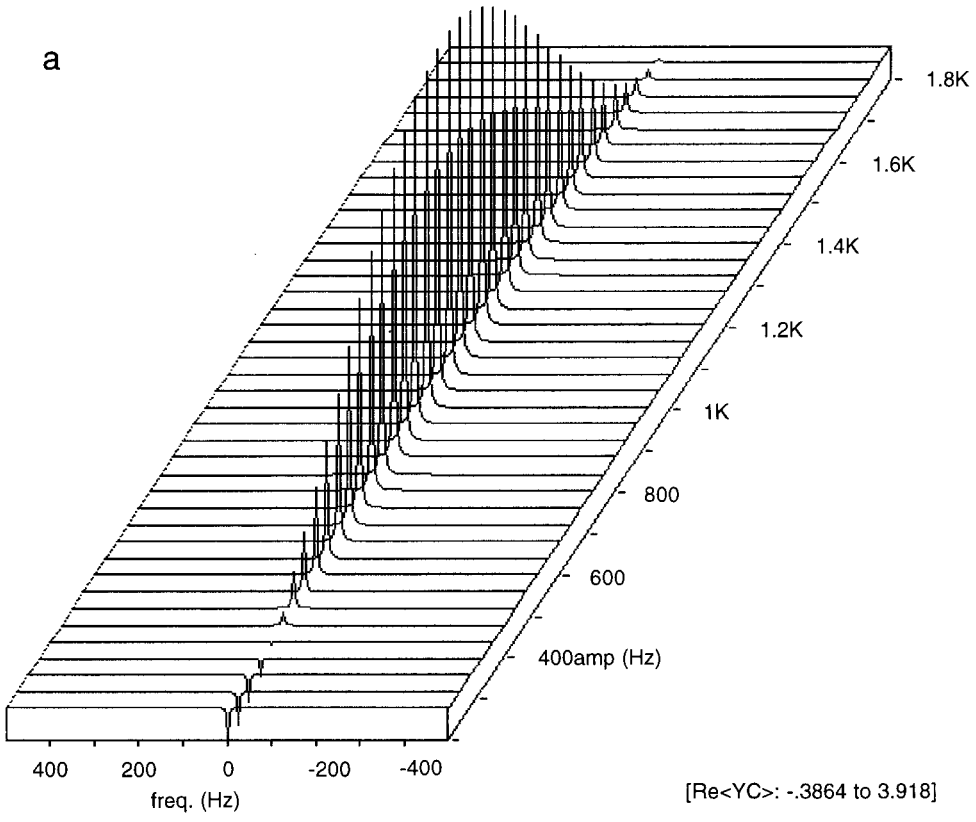
a
1.8K
1.6K
1.4K
1.2K
1K
800
600
400amp (Hz)
400
200
0
-200
-400
freq. (Hz)
[Re<YC>: -.3864 to 3.918]

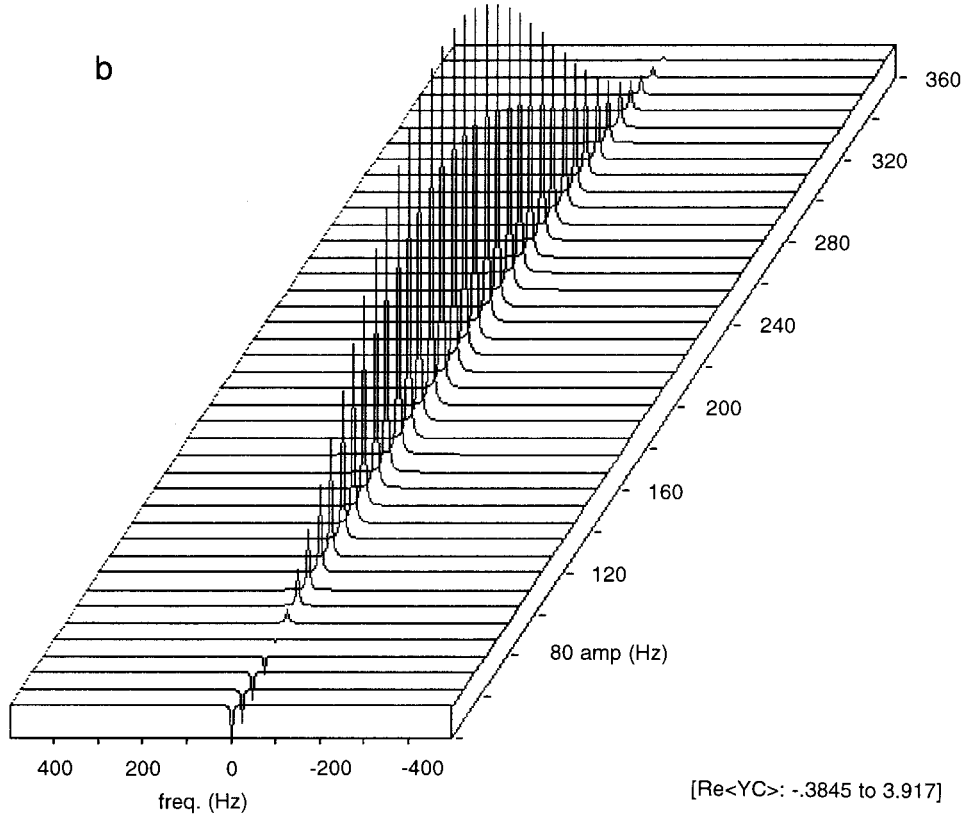
b
360
320
280
240
200
160
120
80 amp (Hz)
400
200
0
-200
-400
freq. (Hz)
[Re<YC>: -.3845 to 3.917]

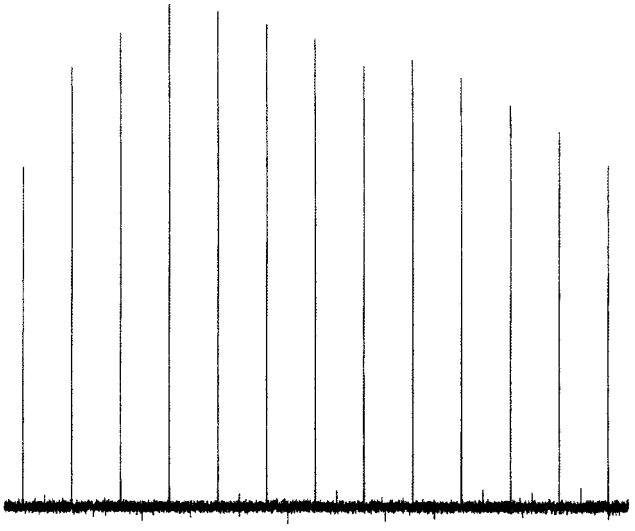

FIG. 5. Signal amplitude obtained with PRAWN-π in forward mode on sodium [2-^{13}C]acetate, as a function of proton attenuator setting, varied from 13.0 to 25.0 dB in 1.0-dB steps. The π pulse width was 500 μs; all other parameters as in caption to Fig. 3.

$$+\frac{4k(1-c)}{(4k^2+1)}(I_yS_y+I_zS_z)$$

$$+\frac{2s}{(4k^2+1)^{1/2}}(I_yS_z-I_zS_y). \qquad [8]$$

The transformation of I_x under the Hamiltonian of Eq. [6] is thus given by (*17*)

$$I_x \xrightarrow{\bar{H}t} \frac{(1+8k^2+c)}{2(4k^2+1)}I_x+\frac{(1-c)}{2(4k^2+1)}S_x$$

$$+\frac{2k(1-c)}{(4k^2+1)}(I_yS_y+I_zS_z)$$

$$+\frac{s}{(4k^2+1)^{1/2}}(I_yS_z-I_zS_y). \qquad [9]$$

As against this behavior, we may compute the evolution of the relevant density matrix components under the mismatch compensated sequence described earlier. We note first that for the transformation of the relevant symmetric density operator component under this sequence, we have, owing to the action of the π pulse pair,

$$(I_x+S_x) \xrightarrow{t} -(I_x+S_x). \qquad [10]$$

For the evolution of the corresponding antisymmetric component, we have

$$(I_x-S_x) \xrightarrow{(CP)_x,\ t/2} \frac{(4k^2+c')}{(4k^2+1)}(I_x-S_x)$$

$$+\frac{4k(1-c')}{(4k^2+1)}(I_yS_y+I_zS_z)$$

$$+\frac{2s'}{(4k^2+1)^{1/2}}(I_yS_z-I_zS_y)$$

$$\xrightarrow{\pi_y(I,S)} -\frac{(4k^2+c')}{(4k^2+1)}(I_x-S_x)$$

$$+\frac{4k(1-c')}{(4k^2+1)}(I_yS_y+I_zS_z)$$

$$-\frac{2s'}{(4k^2+1)^{1/2}}(I_yS_z-I_zS_y)$$

$$\xrightarrow{(CP)_x,\ t/2} \left[-\frac{(4k^2+c')^2}{(4k^2+1)^2}+\frac{s'^2}{(4k^2+1)}\right.$$

$$\left.+\frac{4k^2(1-c')^2}{(4k^2+1)^2}\right](I_x-S_x)+\cdots$$

$$\equiv -\frac{(16k^4-8k^2+16k^2c'+c)}{(16k^4+8k^2+1)}$$

$$\times(I_x-S_x)+\cdots. \qquad [11]$$

We thus find for the transformation of I_x under the mismatch compensated sequence:

$$I_x \xrightarrow{t} -\frac{(1+32k^4+16k^2c'+c)}{2(16k^4+8k^2+1)}I_x$$

$$-\frac{(1+16k^2-16k^2c'-c)}{2(16k^4+8k^2+1)}S_x+\cdots. \qquad [12]$$

The trigonometric coefficients that occur in Eqs. [8] to [12] are defined as follows:

$$c=\cos(\pi J(4k^2+1)^{1/2}t); \quad s=\sin(\pi J(4k^2+1)^{1/2}t);$$

$$c'=\cos\left(\pi\frac{J}{2}(4k^2+1)^{1/2}t\right). \qquad [13]$$

The mismatch compensated sequence thus clearly leads to two frequencies of evolution of the magnetization, one corresponding to the normal frequency of Eq. [9] and another at half this value, the amplitude at this latter frequency vanishing at zero mismatch. The sequence brings about its compensating effect by "rephasing" the terms corresponding to in-phase and anti-phase antisymmetric components of the density operator,

as seen from Eq. [10]. Mismatch compensation by the π pulses is 100% effective for k upto $\frac{1}{2}$, declining to 64% for $k = 1$; the PRAWN-π mode of operation amplifies this range as discussed earlier.

J CROSS-POLARIZATION UNDER OFF-RESONANCE CONDITIONS

Finally, we consider the general off-resonance case, with resonance offsets δ. We recall that the Hamiltonian of *J* cross-polarization in this case takes the following well-known forms in the doubly rotating frame (DRF) and tilted doubly rotating frame (TDRF) (*6*):

$$\begin{aligned} H_{\mathrm{DRF}} &= \delta_I I_z + \delta_S S_z + \omega_{1I} I_x + \omega_{1S} S_x + 2\pi J I_z S_z \\ H_{\mathrm{TDRF}} &\equiv H_T = THT^{-1} \\ &= \exp(\mathbf{i}\theta_I I_y)\exp(\mathbf{i}\theta_S S_y)\, H\, \exp(-\mathbf{i}\theta_S S_y)\exp(-\mathbf{i}\theta_I I_y) \\ &\quad \times \left(\tan\theta = \frac{\omega_1}{\delta}\right). \end{aligned} \qquad [14]$$

For the Hamiltonian in the synchronized, tilted doubly rotating frame, we have (*6*)

$$\begin{aligned} H_{\mathrm{STDRF}} &= \exp\left(-\frac{\mathbf{i}}{2}(\Omega_I + \Omega_S)(I_z + S_z)t\right) \\ &\quad \times H_T \exp\left(\frac{\mathbf{i}}{2}(\Omega_I + \Omega_S)(I_z + S_z)t\right) \\ &= \tfrac{1}{2}(\Omega_I - \Omega_S)(I_z - S_z) \\ &\quad + 2\pi J(c_{\theta_I}c_{\theta_S} I_z S_z + \tfrac{1}{2} s_{\theta_I} s_{\theta_S}(I_x S_x + I_y S_y)); \\ &\equiv H_{\mathrm{I}} + H_{\mathrm{II}} \\ (\Omega &= (\omega_1^2 + \delta^2)^{1/2}) \\ H_{\mathrm{I}} &= \pi J s_{\theta_I} s_{\theta_S}[(I_x S_x + I_y S_y) + k(I_z - S_z)]; \\ k &= \frac{(\Omega_I - \Omega_S)}{2\pi J s_{\theta_I} s_{\theta_S}} \\ H_{\mathrm{II}} &= 2\pi J c_{\theta_I} c_{\theta_S} I_z S_z. \end{aligned} \qquad [15]$$

The last form, involving partitioning into two commuting terms, is valid only for the two-spin-$\frac{1}{2}$ system.

The total angular momentum component along the effective field direction is conserved under this Hamiltonian, which we now write without the subscripts:

$$[H,\, I_z + S_z] = [I_x S_x + I_y S_y,\, I_z + S_z] = 0. \qquad [16]$$

Taking note of the relevant commutator algebra, we find for the integrated equation of motion of I_z

$$\begin{aligned} I_z \rightarrow & \frac{(1 + 8k^2 + c_2)}{2(4k^2 + 1)} I_z + \frac{(1 - c_2)}{2(4k^2 + 1)} S_z \\ & + \frac{2k(1 - c_2)}{(4k^2 + 1)} (I_x S_x + I_y S_y) \\ & + \frac{s_2}{(4k^2 + 1)^{1/2}} (I_x S_y - I_y S_x). \end{aligned} \qquad [17]$$

Note that Eq. [17] is identical in form to Eq. [9]: the antisymmetric $(I_z - S_z)$ term in the STDRF commutes with H_{II}. Note further that Eq. [17] includes three observable *S* spin terms, upon taking into account the reverse synchronization and tilt transformations: S_z, $I_x S_x$, and $I_x S_y$.

On the other hand, we find for I_x the transformation

$$\begin{aligned} I_x \rightarrow & c_1 c_3 I_x + 2 c_1 s_3 I_y S_z \\ & + \frac{2 s_1 c_3}{(4k^2 + 1)^{1/2}} (k I_y - I_z S_y) \\ & + \frac{4 s_1 s_3}{(4k^2 + 1)^{1/2}} \left(\frac{1}{4} S_x - k I_x S_z\right). \end{aligned} \qquad [18]$$

Equation [18] includes in turn three further "observable" *S* spin terms (but see below): S_x, $I_x S_z$, and $I_z S_y$.

In the above, the frequencies denoted with the subscripts 1, 2 and 3 arise respectively from the Hamiltonian terms H_{I}, H_{I} and H_{II}. The various trigonometric coefficients that occur in Eqs. [17] and [18] correspond to

$$\begin{aligned} c_1 &= \cos\left(\pi \frac{J}{2} s_{\theta_I} s_{\theta_S} (4k^2 + 1)^{1/2} t\right) \\ s_1 &= \sin\left(\pi \frac{J}{2} s_{\theta_I} s_{\theta_S} (4k^2 + 1)^{1/2} t\right) \\ c_2 &= \cos(\pi J s_{\theta_I} s_{\theta_S} (4k^2 + 1)^{1/2} t) \\ s_2 &= \sin(\pi J s_{\theta_I} s_{\theta_S} (4k^2 + 1)^{1/2} t) \\ c_3 &= \cos(2\pi J c_{\theta_I} c_{\theta_S} t); \quad s_3 = \sin(2\pi J c_{\theta_I} c_{\theta_S} t). \end{aligned} \qquad [19]$$

Taking into account the reverse transformations corresponding to synchronization and tilt, and neglecting as unobservable the signal contributions from Eq. [18] invoking dephasing under RF field inhomogeneities (*5, 6*), we now arrive

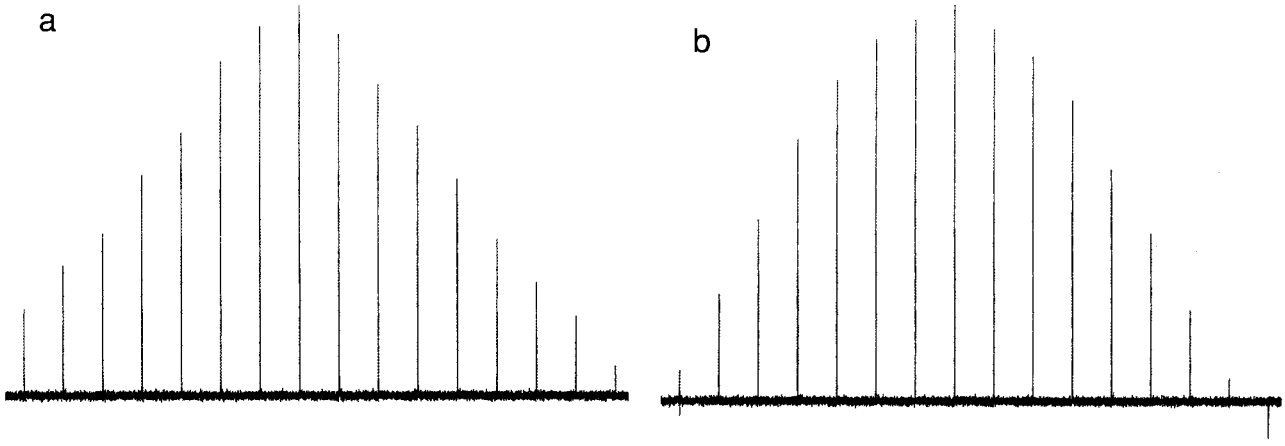

FIG. 6. (a) Signal amplitude obtained with PRAWN in forward mode on sodium [2-^{13}C]acetate, as a function of ^{1}H resonance offset. The carbon spin was irradiated on resonance (9685 Hz). ^{1}H resonance offset was stepped through resonance (29747 Hz), from 29552 to 30002 Hz in 30-Hz steps. The carbon attenuator was set to 10 dB and the proton attenuator to 17.5 dB, corresponding nominally to 1 kHz peak RF amplitude on each channel. All other parameters as in caption to Fig. 3. (b) Signal amplitude obtained with PRAWN-π in forward mode on sodium [2-^{13}C]acetate, as a function of ^{1}H resonance offset, stepped through resonance (29747 Hz) from 29552 to 30002 Hz in 30-Hz steps. The carbon spin was irradiated on resonance. The π pulse width was 500 μs; all other parameters as in (a).

finally at the following expression for the S spin signal intensity **S**:

$$\mathbf{S} \sim \frac{\sin\theta_S \sin\theta_I}{2(4k^2+1)}(1-c_2)S_x - \frac{2k\cos\theta_S \sin^2\theta_I}{(4k^2+1)}(1-c_2)I_zS_x - \frac{\sin^2\theta_I}{(4k^2+1)^{1/2}}s_2I_zS_y. \quad [20]$$

It follows from the form of H_1 in Eq. [15] that the π pulse pair has the same mismatch compensating effect in this case, so that we have for the I decoupled S spin signal arising from the mismatch compensated sequence (of duration t) in the off-resonance case:

$$\mathbf{S} \sim -\frac{(1+16k^2-16k^2c_1-c_2)}{2(16k^4+8k^2+1)}\sin\theta_S \sin\theta_I. \quad [21]$$

The sequence thus compensates Hartmann–Hahn mismatch while retaining the signal dependence on resonance offset in terms of the tilt parameters. This appears to be an attractive characteristic especially suited for the imaging applications in view, since in practice this implies retention of selectivity in polarization transfer, while compensating for mismatch, including effects of field drifts which are sensed in proportion to γ. The behavior of PRAWN and PRAWN-π as a function of proton resonance offset is exhibited in Figs. 6a and 6b.

DISCUSSION

In operation, we have employed both versions of PRAWN with satisfactory results on AX, AX_2, and AX_3 spin systems with $^{1}J_{\text{C-H}}$ in the range 120–165 Hz, and on an AX_2 system with $^{2}J_{\text{C-H}} \approx 2.3$ Hz, as well as on elastomers and on plants *in vivo*. In the cases with transfer mediated by one-bond couplings, we typically cover the mixing period with one PRAWN cycle, pulsing at the rate of 4 to 10 kHz; for the version with the π pulse pair, it then proves quite satisfactory to locate the pulse pair midway through the cycle. We have to date found the sequences to work reliably on both single-coil and two-coil 5- and 10-mm probeheads, as well as on 25-mm resonators, 25-cm resonators, and a quadrature head coil (^{1}H)/surface coil (^{13}C) system. The merits of the PRAWN family of sequences are their ease of implementation, their insensitivity to mismatch of the contact pulse amplitudes, and their efficiency even at extremely low duty cycles.

ACKNOWLEDGMENTS

The doubly tuned single coil probehead inserts employed in part of this work were built by M. Heidenreich. The tests on 25-cm resonators and head coil systems were performed at the Magnetic Resonance Center, University of Nottingham. The authors have great pleasure in acknowledging the friendly cooperation of M. Heidenreich and Dr. A. Spyros and discussions with them, as well as technical assistance from K. Gille and H. Wiringer. N.C. acknowledges stimulating interaction with Prof. P.G. Morris, Dr. R. Bowtell, Dr. W. Köckenberger, and Mr. R. Mann, and especially the kind help of Prof. J.S. Waugh in sending him a copy of Antiope. N.C. gratefully acknowledges the Deutsche Forschungsgemeinschaft for grant of a Gastprofessur and CSIR for deputing him on the visit.

REFERENCES

1. C. Kunze and R. Kimmich, *J. Magn. Reson. B* **105,** 38–44 (1994).
2. M. Heidenreich, W. Köckenberger, R. Kimmich, N. Chandrakumar, and R. Bowtell, *J. Magn. Reson.* **132,** 109–124 (1998).
3. A. Spyros, N. Chandrakumar, M. Heidenreich, and R. Kimmich, *Macromolecules* **31,** 3021–3029 (1998).
4. S. R. Hartmann and E. L. Hahn, *Phys. Rev.* **128,** 2042–2053 (1962).
5. L. Müller and R. R. Ernst, *Molec. Phys.* **38,** 963–992 (1979).
6. G. C. Chingas, A. N. Garroway, R. D. Bertrand, and W. B. Moniz, *J. Chem. Phys.* **74,** 127–156 (1981).
7. G. C. Chingas, A. N. Garroway, R. D. Bertrand, and W. B. Moniz, *J. Magn. Reson.* **35,** 283–288 (1979).
8. N. Chandrakumar and K. Nagayama, *Chem. Phys. Lett.* **133,** 288–292 (1987).
9. M. H. Levitt, *J. Chem. Phys.* **94,** 30–38 (1991).
10. S. J. Glaser and J. J. Quant, *Adv. Magn. Reson.* **19,** 59–252 (1996).
11. J. D. Ellett, Jr., and J. S. Waugh, *J. Chem. Phys.* **51,** 2851–2858 (1969).
12. J. S. Waugh, *J. Magn. Reson.* **96,** 286–289 (1992).
13. N. Chandrakumar, XI International Conference on Magnetic Resonance in Biological Systems, Goa (1984); N. Chandrakumar, *J. Magn. Reson.* **63,** 202–206 (1985).
14. Ē. Kupče and R. Freeman, *J. Am. Chem. Soc.* **114,** 10671–10672 (1992).
15. R. Konrat, I. Burghardt, and G. Bodenhausen, *J. Am. Chem. Soc.* **113,** 9135–9140 (1991).
16. H. Kessler, C. Griesinger, R. Kerssebaum, K. Wagner, and R. R. Ernst, *J. Am. Chem. Soc.* **109,** 607–609 (1987).
17. N. Chandrakumar, *J. Magn. Reson.* **67,** 457–465 (1986).